Environ. Sci. Technol. **2009,** *43,* 5940–5946

Airborne Virus Capture and Inactivation by an Electrostatic Particle Collector

ERIC M. KETTLESON,[†] BALA RAMASWAMI,[†] CHRISTOPHER J. HOGAN, JR.,[†] MYONG-HWA LEE,[‡] GENNADIY A. STATYUKHA,[§] PRATIM BISWAS,[†] AND LARGUS T. ANGENENT*,[||]

Department of Energy, Environmental and Chemical Engineering, Washington University in St. Louis, St. Louis, Missouri 63130, Environmental and Energy Division, Korea Institute of Industrial Technology, CheonAn City, South Korea, Cybernetics of Chemical Technology Processes, National Technical University of Ukraine, Kiev, Ukraine, and Department of Biological and Environmental Engineering, Cornell University, 214 Riley-Robb Hall, Ithaca, New York 14853

Received November 20, 2008. Revised manuscript received May 19, 2009. Accepted June 2, 2009.

Airborne virus capture and inactivation were studied in an electrostatic precipitator (ESP) at applied voltages from −10 to +10 kV using aerosolized bacteriophages T3 and MS2. For each charging scenario, samples were collected from the effluent air stream and assayed for viable phages using plaque assays and for nucleic acids using quantitative polymerase chain reaction (qPCR) assays. At higher applied voltages, more virus particles were captured from air with maximum log reductions of 6.8 and 6.3 for the plaque assay and 4.2 and 3.5 for the qPCR assay at −10 kV for T3 and MS2, respectively. Beyond corona inception (i.e., at applied voltages of −10, −8, +8, and +10 kV), log reduction values obtained with the plaque assay were much higher compared to those of the qPCR assay because nonviable particles, while present in the effluent, were unaccounted for in the plaque assay. Comparisons of these assays showed that in-flight inactivation (i.e., inactivation without capture) was greater for the highest applied voltages with a log inactivation of 2.6 for both phages at −10 kV. We have demonstrated great potential for virus capture and inactivation via continual ion and reactive species bombardment when conditions in the ESP are enforced to generate a corona discharge.

Introduction

According to the World Health Organization, the most prevalent transmissible diseases in the world are respiratory infections (*1*). These infections, originating from bacterial or viral exposure, may be transmitted in indoor environments via a number of different ways, including direct or indirect contact with an infected surface, droplet transmission, or aerosol transmission (*2*). Aerosol transmission is defined as host inhalation of infectious nuclei (<5 μm in diameter) that have remained suspended in air and disseminated throughout an indoor environment (*3*). Considering that the average person in the United States spends nearly 87% of his time indoors (*4*), maintaining a clean indoor-air environment is an important avenue for mitigating aerosol transmission of respiratory infections.

Engineering controls employed in air handling systems aim to effectively collect/remove aerosol particles from the air stream, utilizing various capture mechanisms depending on the technology used. High-efficiency particulate air (HEPA) filtration can be used to remove airborne particles of biological origin (i.e., bioaerosols) in many indoor environments, including hospitals, office buildings, and aircraft cabins. However, implementation of HEPA filtration bears excessive operational costs because of regular filter replacement and additional power requirements for air recirculation due to a large pressure drop across the filter material. In addition, the filter itself may provide a growth habitat for bacteria (*5*). Coal-fired power plants have circumvented the excessive operational costs by employing electrostatic precipitators (ESPs) to efficiently control fine, nonbiological particle emissions. ESPs have also been placed in household air-forced heating and cooling systems to control aerosol levels. Recently, this particle collection technology has been extensively promoted as a stand-alone "air purifier" to control household bioaerosols.

ESPs consist of charging and collecting electrodes with a negative or positive potential difference between them to create an electric field. Typically, a high voltage is applied to a thin wire (acting as the central charging electrode) to generate ions in an electric field, which collide with and charge the aerosol particles (*6*). Charged aerosol particles migrate toward the oppositely charged collecting electrode, which typically consists of a stainless-steel cylinder or plate. The magnitude of the attractive force on charged particles is proportional to the voltage applied to the charging electrode (*7*). At low to moderate applied voltages, only small quantities of electrons flow to the positive electrode. As the applied voltage increases, the corresponding increase in electric field strength accelerates the flow of electrons. When sufficient kinetic energy is gathered, the collision of an electron with an atom or a gas molecule produces an ion and an additional free electron. Further collisions will generate more ions and free electrons, eventually leading to an exponential increase in the number of free electrons. The high level of ions associated with this phenomenon is characteristic of a corona discharge (*8*), which allows for efficient charging and capture of airborne particles.

The usefulness of ESP technology in mitigating biological aerosols has been demonstrated using both bacterial endospores and various bacterial species (*9, 10*). Other published research involving electrostatic precipitation of bioaerosols has focused almost exclusively on the sampling efficiency of bacterial cells and spores for exposure assessment and their survival rates (i.e., bioavailability) after electrical charging (*11*−*15*). Similarly, the few studies on virus particle behavior in ESPs have only focused on sampling efficiency and not on mitigation effectiveness (*16*−*18*). In addition, a recent paper has combined ESP with biosensors to monitor airborne virus particles (*19*). ESPs have size-dependent collection efficiencies, and while overall mass-based collection efficiencies may be high (e.g., 99%), the collection efficiencies of particles in the submicrometer and

* Corresponding author tel: +1-607-255-2480; fax: +1-607-255-4080; e-mail: la249@cornell.edu.
[†] Washington University in St. Louis.
[‡] Korea Institute of Industrial Technology.
[§] National Technical University of Ukraine.
[||] Cornell University.

10.1021/es803289w CCC: $40.75

Published on Web 06/23/2009

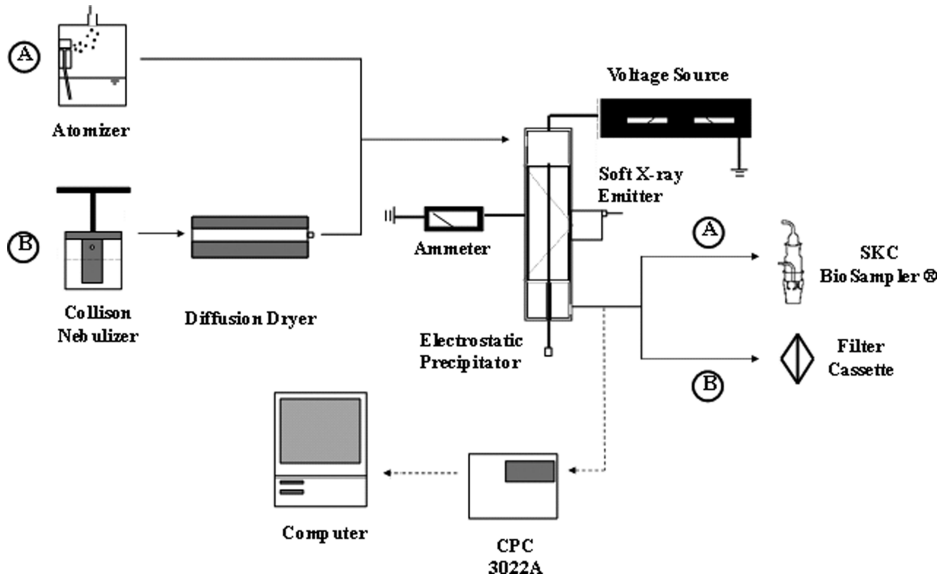

FIGURE 1. Experimental setup for the aerosolization and electrostatic treatment of bacteriophages T3 (path A) and MS2 (path B). Total particle concentration measurements of the ESP effluent air stream are depicted by dashed lines.

nanometer particle size range are typically low (*20*−*23*). Many virus particles are in the submicrometer and nanometer size ranges. The potential to capture such biological particles with high efficiency, and potentially inactivate them in an ESP system has considerable practical importance.

Besides our initial report on physical measurements of particle capture (*24*), the effectiveness of ESPs as an engineering mitigation control for inactivation of airborne virus particles has not been investigated. Thus, the objective of this study was to quantify the capture and inactivation of airborne virus particles using electrostatic precipitation under different operating conditions. To further understand virus collection and inactivation, a soft X-ray enhanced ESP was used in this study (*20, 24, 25*). Previous research has shown that nonbiological nanoparticles (i.e., particles up to 100 nm in size) are difficult to charge in conventional ESPs (*23*), and that soft X-ray irradiation aids in charging such particles by producing additional bipolar ions and also by direct photoionization (*20, 26*). Respiratory infection in humans can be caused by a diverse assortment of viruses, and therefore we propagated and aerosolized both dsDNA and ssRNA viruses, bacteriophages T3 and MS2, with diameters of 45 and 25 nm, respectively. Two assays were used to quantify reduction of bacteriophages T3 and MS2 from the aerosol stream: a plaque assay, which measured the number of viable (i.e., plaque forming) phages in the effluent aerosol and a qPCR assay, which quantified the total nucleic acid mass for both active and inactive T3 and MS2 in the effluent aerosol. PCR-based methods for quantifying airborne microorganisms have been used to assay aerosol samples (*27*), and have been incorporated in recent work relating to bacterial (*28*) and viral aerosols (*29*). From the plaque and qPCR assays, we determined the number of viable phages relative to total phages exiting the system, thereby distinguishing between physical capture and inactivation. Based on these results, mechanisms of viral inactivation within the ESP are discussed.

Materials and Methods

Propagation of Bacteriophages T3 and MS2. Bacteriophages T3 (ATCC 11303-B3) and MS2 (ATCC 15597-B1) were propagated using *Escherichia coli* strain C (ATCC 13706) and strain C-3000 (ATCC 15597) as their respective hosts. The growth media used for *E. coli* strain C was LB broth (Sigma-Aldrich, St. Louis, MO) amended with $CaCl_2$ (Fisher, Pittsburgh, PA) and $MgSO_4$ (Sigma-Aldrich) [per L of deionized water: 20 g of LB broth, 10 mL of 1.0 M $MgSO_4$, and 1.5 mL of 1.0 M $CaCl_2$], while minimal media [per L of deionized water: 100 mL of 10X M9 mix, 10 mL of 10% glucose (Fisher); 10 mL of 1% thiamine (Sigma-Aldrich), and 1 mL of 1.0 M $MgSO_4$] was used to culture *Escherichia coli* strain C-3000. To generate the necessary large-volume, high-titer bacteriophage stock solutions, a 3-day liquid-culture technique (see Supporting Information (SI)) was used. We prepared single high-titer stock solutions for both bacteriophages T3 and MS2 to maintain consistency between experiments. Stock solution concentrations were 1.2×10^9 PFU mL^{-1} and 2.0×10^{10} PFU mL^{-1} for bacteriophages T3 and MS2, respectively. The stock solutions were prepared at the beginning of the study and stored at 4 °C. Before every experimental run, 10 mL of the stock solution was mixed with 55 mL of DI water to make a diluted working solution (1.8×10^8 PFU mL^{-1} and 3.1×10^9 PFU mL^{-1} for bacteriophages T3 and MS2, respectively), which would then be used for aerosolization.

Aerosolization. Different aerosolization techniques were used for T3 and MS2 bacteriophages: a constant output stainless steel atomizer was used for bacteriophage T3 to prevent excessive foaming of its specific broth; a 6-jet Collison nebulizer was used for bacteriophage MS2 to maintain consistency between this study and our preliminary work with MS2 (*24*). Bacteriophage T3 was aerosolized using a constant output atomizer (model 3076, TSI, Inc., St. Paul, MN) containing 65 mL of bacteriophage T3 working solution (Figure 1, path A). The atomizer was operated at an upstream pressure of 240 kPa at a flow rate of 3.0 L min^{-1}, and generated an aerosol with an average number concentration of 9.3×10^6 particles cm^{-3}, a geometric mean diameter (GMD) of 41.3 nm, and a geometric standard deviation (GSD) of 1.82. Particle number concentration, GMD, and GSD were measured using a differential mobility analyzer (model 3081 in Electrostatic Classifier model 3080, TSI Inc., Minneapolis, MN) and an ultrafine condensation particle counter (model 3022a, TSI Inc.) operating together as a scanning mobility particle spectrometer (*30*). HEPA-filtered compressed air at a flow rate of 9.5 L min^{-1} was bubbled through a glass impinger (Ace Glass Inc., Vineland, NJ) containing 10 mL of DI water and combined with the output of the atomizer to further humidify and dilute the air stream to prevent drying and inactivating bacteriophage T3 (*31*). The bacteriophage-laden, humidified aerosol stream was then delivered at a total flow rate of 12.5 L min^{-1} to the inlet of a soft X-ray

enhanced ESP. The soft X-ray enhanced ESP used in this study was designed and built in-house and has been described elsewhere (*20, 24*). Further details can be found in the SI. The atomizer and ESP were connected in series through 3/8 in. I.D. flexible Tygon tubing.

Bacteriophage MS2 was aerosolized using a 6-jet Collison nebulizer (CN-25, BGI Inc., Waltham, MA) containing 65 mL of bacteriophage MS2 working solution (Figure 1, path B). The nebulizer was operated at a flow rate of 7 L min^{-1} by means of a mass flow controller (MKS Instruments, Willmington, MA), and generated an aerosol with an average number concentration of 3.4×10^6 particles cm^{-3}, a geometric mean diameter of 35.7 nm, and a geometric standard deviation of 1.87. HEPA-filtered compressed air at a flow rate of 3.0 L min^{-1} was combined with the output of the nebulizer to dilute the air stream. The bacteriophage-laden aerosol stream was then passed through a diffusion dryer (TSI, St. Paul, MN), and delivered at a total flow rate of 10 L min^{-1} to the inlet of the soft X-ray enhanced ESP. The nebulizer, diffusion dryer, and ESP were connected in series using 3/8 in. I.D. flexible Tygon tubing.

Experimental Protocol. *Experiment 1.* A potential difference (±0, 4, 6, 8, and 10 kV) was formed across the collecting and discharge electrodes, with and without soft X-ray irradiation, for a total of 18 different charging scenarios. A split-plot design was used to study the 18 charging scenarios. First, all scenarios for one polarity were completed (in a randomized order), followed by all scenarios for the other polarity. Different collection techniques were used for T3 and MS2 bacteriophages: biosamplers were used for bacteriophage T3 to prevent desiccation, and therefore to limit baseline inactivation; glass fiber filters were used for bacteriophage MS2 to maximize sampling efficiencies (MS2 was less susceptible to desiccation). At each charging episode, the entire effluent air stream was passed through a BioSampler (AGI-30, SKC Inc., Eighty Four, PA) containing 20 mL of phosphate buffer solution [PBS, per L of deionized water: 8.0 g of NaCl (Fisher), 0.2 g of KCl (Fisher), 1.44 g of Na_2HPO_4 (Sigma-Aldrich), 0.24 g of KH_2PO_4 (Fisher), and 75 μL of Tween 80 (Fisher)] for a period of 60 min to sample for fugitive T3 bacteriophages (total volume of air sampled was 750 L). PBS from the sampler was immediately used for plaque assays and the remainder was stored at 4 °C for subsequent DNA extraction. To collect fugitive MS2 bacteriophages, the entire effluent air stream was passed through a 47-mm glass fiber filter (Whatman Inc., Florham Park, NJ) for a period of 60 min (total volume of air sampled was 600 L). Ten-fold serial dilutions of the filter extract (details of filter extraction procedure are presented in the SI) were used in infectivity assays, with the remainder stored at −20 °C for subsequent qPCR analysis. The experiments were performed in duplicate with the atomizer/nebulizer fluid replaced with fresh diluted phage stock before every run. The collection electrode was wiped with 70% ethanol after each trial and the system was flushed with clean, dry air for 5−10 min preceding the next trial. Air samples (blanks) were collected following the decontamination process on random occasions to assess carryover contamination, accounting for ~5% of all samples.

Experiment 2. Physical measurements of total particle concentrations (i.e., virus particles constitute only a small percentage of the total particle concentration when aerosolized from diluted media) were also made at the ESP outlet with a condensation particle counter (model 3022a, TSI Inc.). The physical measurements, depicted by dashed lines in the experimental setup (Figure 1), were performed under the same operational conditions as the T3 and MS2 effluent study with additional applied potentials of ± 1, 2, 3, 5, 7, 9 kV.

Plaque Assays. A single-agar-layer plaque technique, adapted from the U.S. Environmental Protection Agency Method 1602 for enumeration of F+ and somatic coliphages (*32*), was used to assay for phage viability (see SI for details). The bacteriophage concentrations in the BioSampler and filter extract were determined by overlaying serial dilutions of these samples on the solidified agar plates, incubating the plates overnight at 37 °C, and then enumerating the plaques.

qPCR Analysis of Bacteriophage T3 and MS2. Details on primer design, nucleic acid extraction, and cDNA preparation are provided in the SI. qPCR for DNA of bacteriophage T3 and the cDNA of MS2 was performed using a one-step qPCR SYBR Green Rox kit (AbGene Inc., Rochester, NY) in 25 μL reaction volumes (per reaction: 1 μL of sample, 0.5 U UDP-N-glycosidase [Invitrogen, Carlsbad, CA], and forward and reverse primers at final concentrations of 0.8 μM each). Reactions were performed in triplicate for both samples and standards. qPCR consisted of heat activation of the *Taq* polymerase for 15 min at 95 °C, followed by 40 cycles of 95 °C for 15 s, 55 °C for 45 s, and 72 °C for 30 s in an Mx3000P system (Stratagene, La Jolla, CA). The limit of detection (i.e., sensitivity) of the qPCR reaction was 2.44 fg of genomic DNA (64 genomic equivalents) and 10 pg of genomic RNA (6020 genomic equivalents) for bacteriophage T3 and MS2, respectively. To generate a standard curve for qPCR, DNA was extracted from a bulk stock of bacteriophage T3 using two rounds of phenol-chloroform extraction, further purified by treatment with RNase (Promega, Madison, WI), and quantified using a PicoGreen dsDNA Quantitation Kit (Molecular Probes, Eugene, OR). Six 10-fold serial dilutions of this DNA, ranging in concentration from 2.44 ng μL^{-1} to 2.44 fg μL^{-1}, were used as standards. Commercial MS2 RNA (Roche Diagnostics, Indianapolis, IN) was used to generate a standard curve. cDNA was prepared from five 10-fold serial dilutions of this RNA, ranging in concentration from 100 ng μL^{-1} to 10 pg μL^{-1}.

Data Analysis. Log reduction was calculated as the log difference between the measured outlet value for the baseline and the experimental conditions:

$$\text{Log reduction} = \log\left(\frac{N_{\text{Baseline}}}{N_{\text{Experiment}}}\right) \quad (1)$$

where N_{Baseline} is the total measured value (i.e., PFUs, mass of DNA or RNA, or total particle concentration) at the baseline condition (i.e., 0 kV applied voltage, X-ray off) and $N_{\text{Experiment}}$ is the measured value at a particular experimental charging scenario. Log inactivation was calculated as the log difference between the total outlet numbers of bacteriophages for the qPCR (i.e., nucleic acid quantification regardless of activity) and the plaque (i.e., active bacteriophage quantification) assays:

$$\text{Log inactivation} = \log\left(\frac{N_{\text{qPCR}}}{N_{\text{PA}}}\right)_{\text{Experiment}} - \log\left(\frac{N_{\text{qPCR}}}{N_{\text{PA}}}\right)_{\text{Baseline}} \quad (2)$$

where N_{qPCR} is the total number of bacteriophages obtained by converting the mass of DNA (or RNA) obtained from the qPCR analysis using molecular weights of 2.3×10^7 g mol^{-1} and 1.0×10^6 g mol^{-1} for T3 dsDNA (*33*) and MS2 ssRNA (*34*), respectively. N_{PA} is the total number of bacteriophages obtained from the plaque assay. Several experimental parameters affect the number of viable phages measured during each experimental trial, such as the relative humidity, loss of sampling liquid, and virus inactivation by drying. However, we fixed these parameters for each trial, including for the baseline conditions. Because our data are expressed as the logarithm of a ratio with a baseline value, the final values are unambiguous. The description of the statistical analyses is given in the SI.

Results and Discussion

Electrostatic Reduction of Viral Aerosols. We define reduction here as the decrease in detectable levels of bacterioph-

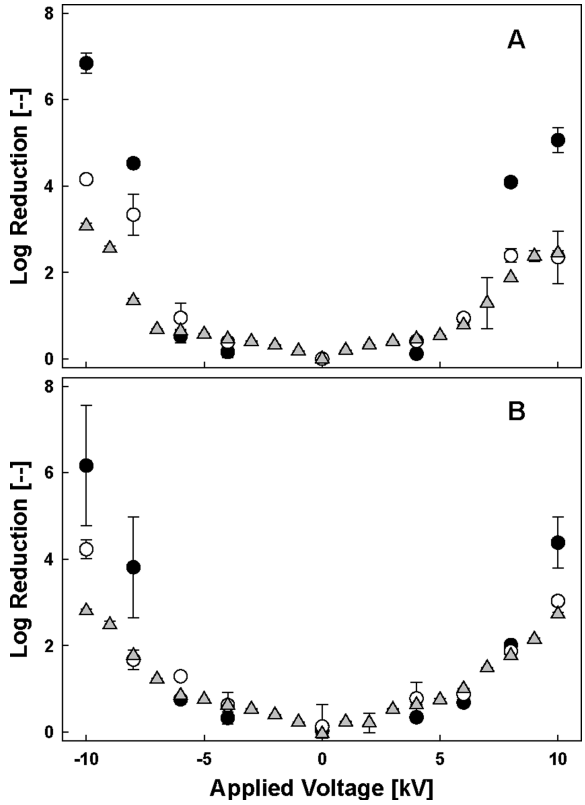

FIGURE 2. Log reduction of bacteriophage T3 without soft X-ray irradiation (A) and with soft X-ray irradiation (B) based on plaque (●), qPCR (○), and total particle concentration (△) measurements of the ESP effluent air stream. For the plaque and qPCR data, points are the mean of duplicate measurements with error bars representing the relative standard deviation. For the total particle concentration data, points are the mean of triplicate measurements, with error bars representing the relative standard deviation.

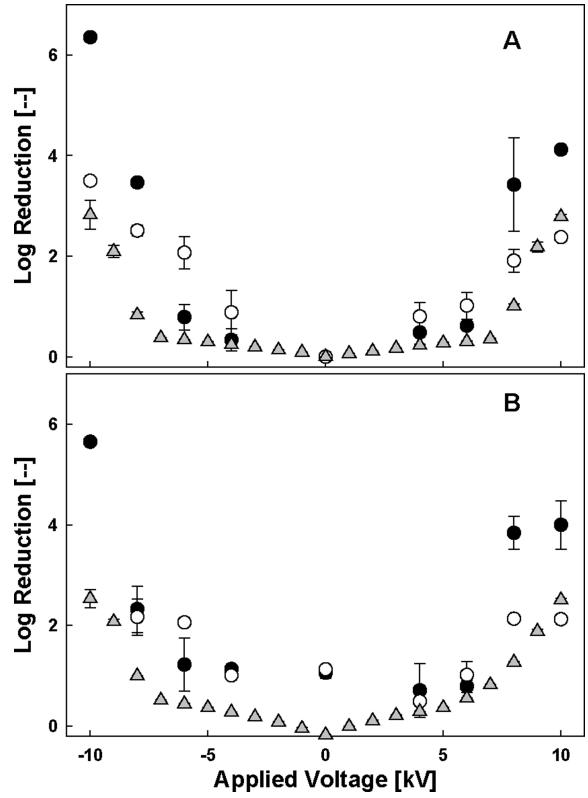

FIGURE 3. Log reduction of bacteriophage MS2 without soft X-ray irradiation (A) and with soft X-ray irradiation (B) based on plaque (●), qPCR (○), and total particle concentration (△) measurements of the ESP effluent air stream. For the plaque and qPCR data, points are the mean of duplicate measurements with error bars representing the relative standard deviation. For the total particle concentration data, points are the mean of triplicate measurements, with error bars representing the relative standard deviation.

ages in the effluent air stream of the ESP when compared to baseline conditions regardless of the method used. As anticipated, reduction of airborne bacteriophage T3 and MS2 significantly increased as the magnitude of applied voltage increased from 0 to −10 kV and from 0 to +10 kV as measured both by the plaque assay ($t_{calc} = 20.6$ for T3 and 18.9 for MS2; $p = 0.1$) and the qPCR assay ($t_{calc} = 22.0$ for T3 and 13.3 for MS2, $p = 0.1$). We obtained U-shaped figures when log reduction was plotted as a function of applied voltage from −10 to 10 kV (Figures 2 and 3). A sharp increase in log reduction values occurred between −6 and −8 kV and between +6 and +8 kV. For example, log reduction for bacteriophage T3 increased from 0.94 to 4.1 and from 0.95 to 2.4 according to the plaque and qPCR assays, respectively, when the applied voltage increased from +6 to +8 kV without X-ray irradiation (Figure 2A). This increase in reduction coincided with the inception of a corona (*20, 24*).

Plaque and qPCR Assays. Log reduction values for both bacteriophage T3 and MS2 did not differ considerably between the plaque and qPCR assays at applied potentials from −6 to +6 kV (Figures 2A and 3A). In this applied potential window (below corona inception), plaque and qPCR log reduction measurements are in agreement with the physical particle measurements from Experiment 2 (Figures 2 and 3) indicating that physical capture within the ESP was the primary mechanism causing bacteriophage reduction. At the highest applied voltages, however, when a corona discharge was present (at −10, −8, +8, and +10 kV; without X-ray irradiation), bacteriophage log reduction values differed considerably between the assays. Maximum bacteriophage T3 log reduction values exceeded 6.8 and 4.2 (i.e., 99.99998% and 99.994%) according to the plaque and qPCR assays, respectively (Figure 2A). For bacteriophage MS2, maximum log reduction values at the highest voltages without X-ray irradiation exceeded 6.3 and 3.5, respectively (Figure 3A). Thus, above corona inception, the plaque assay showed additional reduction, attributable to the presence of inactive virions, which were detectable via qPCR and physical measurements, but not via plaque assays.

Quantitative PCR assay results are not impervious to inactivation mechanisms, especially since ESP environments at high applied voltages may be reactive enough to cause damage to the nucleic acids of virus particles, thereby reducing the nucleic-acid amplification efficiency. Shin and Sobsey (*35*) have shown in their work on virus inactivation with ozone that by increasing the amplicon size, an RT-PCR assay agreed better with a viability assay (plaque assay). The intention of our qPCR assay was the opposite, and therefore we used small amplicon sizes (i.e., 128 and 99 nucleotides for T3 and MS2, respectively) in an effort to reduce the likelihood that nucleic acid damage would interfere with amplification.

To understand if either the plaque assay or qPCR assay can be used solely to study the effects of the factors on log reduction, a correlation analysis between the plaque and nucleic acid log reductions for X-ray on/off, negative or positive potential, and voltage was performed, which showed that the influence of these significant factors on the log reduction change was identical (overall $R = 0.8$). Clearly, either infectivity or nucleic acid-based techniques can be used to study the effects. However, using both methods in

TABLE 1. Effective Log Inactivation of Bacteriophages T3 and MS2 in the Effluent Air Stream Based on Total Number of Phages Derived from qPCR and Plaque Assays[a]

	bacteriophage T3		bacteriophage MS2	
applied voltage [kV]	X-ray OFF	X-ray ON	X-ray OFF	X-ray ON
−10	2.63 (0.30)	0.93 (0.80)	2.63 (na)	na
−8	1.40 (0.41)	1.33 (0.52)	0.97 (0.18)	0.09 (0.47)
−6	−0.33 (0.38)	−0.11 (0.22)	−1.24 (0.37)	−1.09 (0.39)
−4	−0.24 (0.26)	−0.33 (0.39)	−0.41 (0.41)	0.14 (0.15)
0	----	−0.08 (0.36)	----	−0.36 (na)
4	−0.30 (0.22)	−0.29 (0.45)	−0.29 (0.35)	−0.05 (0.39)
6	−0.01 (0.21)	−0.18 (0.42)	−0.32 (na)	−0.17 (0.29)
8	1.73 (0.25)	0.15 (0.37)	0.93 (0.49)	1.59 (0.30)
10	2.96 (0.50)	1.04 (0.43)	1.74 (na)	1.66 (0.37)

[a] Values reported reflect the magnitude of log inactivation obtained at each applied voltage minus the extent of inactivation occurring under baseline conditions (0 kV, X-ray off). Relative standard deviation is included (in parentheses).

this study was useful in the assessment of airborne virus reduction to quantify in-flight inactivation.

Physical measurements of total particle counts included all airborne particles, including salt and macromolecules from the broth, while only bacteriophages T3 and MS2 were targeted in the qPCR and plaque assays. Nevertheless, a valid comparison of the data obtained from the qPCR and plaque assays with the physical particle measurements was possible since the virus particles were attached to larger carrier particles and distributed across the spectrum of particle sizes (*31*).

In-Flight Inactivation. We were able to quantify inactivation of fugitive bacteriophages T3 and MS2 by comparing the estimated phage numbers in the effluent samples determined by the qPCR and plaque assays. The highest log inactivation was found at the highest applied voltages. For example, bacteriophage T3 log inactivation without X-ray irradiation was 2.63 at an applied voltage of −10 kV (Table 1). This was the same for bacteriophage MS2, with a log inactivation of 2.63 at an applied voltage of −10 kV (Table 1). Similar to the log reductions, an increase in log inactivation was observed beyond the corona inception point; for bacteriophage T3 without X-ray irradiation, log inactivation increased from −0.01 to 1.73 after the applied voltage was increased from +6 to +8 kV, and from −0.33 to 1.40 after the applied voltage was increased from −6 and −8 kV (Table 1). Before corona inception, at applied voltages between −6 and +6 kV, the bacteriophage T3 log inactivation, without X-ray irradiation, was zero (log inactivation values oscillated between −0.33 and −0.01, but included zero when measurement uncertainty was considered). With virions that were captured on the collection electrode and sampled after a 1-h run, log inactivation also increased considerably above the corona inception point (see SI).

Inactivation Mechanisms. The mechanisms of inactivation were not explicitly investigated in this study, but we theorize here that mechanisms involving reactive species play an important role besides inactivation because of increased charge levels (*24*). Reactive species (including O_3 and various radicals, such as O·, N·, OH·, and HO_2· *36*−*39*) are generated in coronas, which contribute to inactivation. This is consistent with the observation that inactivation increased after corona inception. The ESP used in this study produces a localized plasma (or region of ionized gas) in the immediate vicinity surrounding the stainless steel wire (the discharge electrode). These ions then attach to or interact with gas molecules creating the reactive species.

Reactive species present in corona discharges (*40*) may lead to inactivation through sufficient damage to either the protein or nucleic acid structure of the bacteriophage. The MS2 virion is composed of 180 molecules of a coat protein, a single maturation protein, and a 3569-nucleotide RNA genome (*41, 42*). The maturation protein is known to play a role in host recognition, attachment to the *E. coli* pilus, and infectivity in vivo (*41, 43*). In addition, the MS2 RNA genome also codes for a replicase subunit and a lysis protein (*44, 45*). Direct damage to the coat protein, maturation protein, or portions of the coding regions on the RNA genome could render the virion noninfectious. Studies investigating the effect of corona discharge on dust mite and cat allergens have shown that these allergens, which differ structurally from one another, can be destroyed by exposure to the corona discharge products (*46, 47*). The authors suggest that the active corona products must follow a broad-spectrum method for destroying the proteins, presumably by affecting their primary structure. Similar results were obtained with Japanese cedar pollen (*48*).

The types and quantity of reactive species produced during corona discharge depend on whether the ESP is operated under a negative or positive applied potential (i.e., negative or positive corona, respectively) (*37*−*39*), which could possibly influence the inactivation efficiencies. Indeed, the log reduction values obtained with the negative corona were statistically significantly higher than with the positive corona for both the plaque and nucleic acid assays ($t_{calc} = 2.94$ and 3.93 for bacteriophage T3 and $t_{calc} = 2.24$ and 6.59 for MS2, respectively; $p = 0.1$). Further studies are required to investigate inactivation mechanisms on a molecular level in ESPs operated with a high-applied voltage.

Soft X-ray Irradiation. Previous research has shown that nonbiological nanoparticles (i.e., particles up to 100 nm in size) are difficult to charge in conventional ESPs (*23*), and that soft X-ray irradiation aids in charging such particles by producing additional bipolar ions and also by direct photoionization (*20, 26*). Soft X-ray irradiation was, therefore, included in these experiments because MS2 virions are ∼25 nm in diameter. However, no statistically significant difference in bacteriophage MS2 log reduction was found with and without X-ray irradiation for the plaque and nucleic acid assays ($t_{calc} = 0.06$ and 0.79, respectively, $p = 0.1$) when a corona was present. For bacteriophage T3, a small but significant difference was found for the plaque assay log reduction ($t_{calc} = 2.66$, $p = 0.1$), but not the nucleic acid log reduction ($t_{calc} = 1.45$, $p = 0.1$). This significant difference for bacteriophage T3 was the result of lower inactivation values at applied voltages beyond corona inception. The discussion for these results is given in the SI.

Particle size distributions of aerosolized viruses, obtained from real-time physical measurements, have shown that most were attached to carrier particles and that the average virus-containing particle was greater than 100 nm in size (*31*). The minor effects that soft X-ray irradiation was found to have on log reduction in this study may be, in part, a consequence of virus particle attachment to larger carrier particles. However, if in indoor environments the sizes of airborne virus particles are within the penetration window of conventional ESPs, soft X-ray enhanced ESPs may enhance virus capture. In addition, soft X-ray enhancement may be useful for larger, but difficult to charge biological particles by direct photoionization. Furthermore, the presence of soft X-ray irradiation reduces the corona inception voltage (*24*), which is of practical importance in such devices.

Future Considerations. We have shown that corona formation in ESPs is essential for considerable capture and in-flight inactivation of virus particles. HEPA filtration can also capture virus particles, but ESPs protect the indoor environment without regular filter maintenance and associ-

ated pressure drop concerns. UV irradiation can inactivate virus particles while in flight, but without a capture mechanism. Indoor air is composed of a host of biological particles, including viruses, bacteria, bacterial and fungal spores, and pollen. The ability of ESPs to eliminate the exposure potential of, for example, spores and pollen that can retain their infectious/allergenic properties even after UV irradiaiton, as well as provide biological inactivation, is a powerful benefit of ESP technology compared to stand-alone UV irradiation technology. However, the formation of ozone must be monitored carefully because it could pose a concern. The combination of capture and inactivation for ESP technology is shared with hybrid mitigation technologies, such as HEPA-UV systems. Further work should be initiated to broaden our study and to compare capture and inactivation efficiencies of ESPs with other mitigation alternatives under different environmental conditions, such as relative humidity. The power consumption for the different technologies should then also be compared.

Bacteriophages were chosen as microbial targets in this study due to the ease with which they could be handled, propagated, and titered, in addition to worker safety concerns. To definitively demonstrate the usefulness of this technology in potential real-life situations, research must be conducted to assess the ability of a soft X-ray enhanced ESP to effectively treat aerosol streams laden with human or animal viruses. The protein and nucleic acid components of these viruses interact with ozone and other reactive species similarly compared to bacteriophages. However, the added structural complexity of outer lipoprotein envelopes of certain animal viruses, such as influenza and poxviruses, compared to bacteriophages, may influence overall inactivation rates considerably. Animal exposure studies incorporating soft X-ray enhanced ESP control technology are ongoing with ectromelia virus (a surrogate for variola virus) and influenza A virus, in addition to other pathogenic microorganisms, such as certain bacteria and bacterial endospores.

Acknowledgments

This work was supported by NIH grant U54 AI057160 to the Midwest Regional Center of Excellence for Biodefense and Emerging Infectious Diseases Research (MRCE). Geoffrey I. Gordon of the Center for Genome Sciences at Washington University Medical School and Justin L. Sonnenburg of the Department of Microbiology and Immunology at Stanford University are acknowledged for their help with qPCR, and Ruth E. Ley of the Department of Microbiology at Cornell University, Jay R. Turner of the Department of Energy, Environmental and Chemical Engineering at Washington University in St. Louis, and anonymous reviewers are acknowledged for their helpful suggestions.

Supporting Information Available

This material is available free of charge via the Internet at http://pubs.acs.org.

Literature Cited

(1) WHO. *Removing obstacles to healthy development: Report on infectious diseases*; World Health Organization, Communicable Diseases Cluster, 1999.
(2) Garner, J. S. Guideline for isolation precautions in hospitals. *Infect. Control Hosp. Epidemiol.* **1996**, *17*, 54–80.
(3) Bridges, C. B.; Kuehnert, M. J.; Hall, C. B. Transmission of influenza: Implications for control in health care settings. *Clin. Infect. Dis.* **2003**, *37*, 1094–1101.
(4) Klepeis, N. E.; Nelson, W. C.; Ott, W. R.; Robinson, J. P.; Tsang, A. M.; Switzer, P.; Behar, J. V.; Hern, S. C.; Engelmann, W. H. The national human activity pattern survey (NHAPS): A resource for assessing exposure to environmental pollutants. *J. Expo. Anal. Environ. Epidemiol.* **2001**, *11*, 231–252.
(5) Kemp, P. C.; Neumeister-Kemp, H. G.; Lysek, G.; Murray, F. Survival and growth of micro-organisms on air filtration media during initial loading. *Atmos. Environ.* **2001**, *35*, 4739–4749.
(6) Friedlander, S. K. *Smoke, Dust, and Haze: Fundamentals of Aerosol Dynamics*, 2nd ed.; Oxford University Press: New York, 2000.
(7) Hinds, W. C. *Aerosol Technology: Properties, Behavior, and Measurement of Airborne Particles*, 2nd ed.; Wiley: New York, 1999.
(8) Crawford, M. *Air Pollution Control Theory*; McGraw-Hill: New York, 1976.
(9) Li, C. S.; Wen, Y. M. Control effectiveness of electrostatic precipitation on airborne microorganisms. *Aerosol. Sci. Technol.* **2003**, *37*, 933–938.
(10) Grinshpun, S. A.; Mainelis, G.; Trunov, M.; Adhikari, A.; Reponen, T.; Willeke, K. Evaluation of ionic air purifiers for reducing aerosol exposure in confined indoor spaces. *Indoor Air* **2005**, *15*, 235–245.
(11) Mainelis, G.; Grinshpun, S. A.; Willeke, K.; Reponen, T.; Ulevicius, V.; Hintz, P. J. Collection of airborne microorganisms by electrostatic precipitation. *Aerosol. Sci. Technol.* **1999**, *30*, 127–144.
(12) Lee, S. A.; Willeke, K.; Mainelis, G.; Adhikari, A.; Wang, H. X.; Reponen, T.; Grinshpun, S. A. Assessment of electrical charge on airborne microorganisms by a new bioaerosol sampling method. *J. Occup. Environ. Hyg.* **2004**, *1*, 127–138.
(13) Mainelis, G.; Willeke, K.; Baron, P.; Reponen, T.; Grinshpun, S. A.; Gorny, R. L.; Trakumas, S. Electrical charges on airborne microorganisms. *J. Aerosol Sci.* **2001**, *32*, 1087–1110.
(14) Mainelis, G.; Gorny, R. L.; Reponen, T.; Trunov, M.; Grinshpun, S. A.; Baron, P.; Yadav, J.; Willeke, K. Effect of electrical charges and fields on injury and viability of airborne bacteria. *Biotechnol. Bioeng.* **2002**, *79*, 229–241.
(15) Yao, M.; Mainelis, G.; An, H. R. Inactivation of microorganisms using electrostatic fields. *Environ. Sci. Technol.* **2005**, *39*, 3338–3344.
(16) Bausum, H. T.; Schaub, S. A.; Kenyon, K. F.; Small, M. J. Comparison of coliphage and bacterial aerosols at a wastewater spray irrigation site. *Appl. Environ. Microbiol.* **1982**, *43*, 28–38.
(17) Harstad, J. B. Sampling submicron T1 bacteriophage aerosols. *Appl. Microbiol.* **1965**, *13*, 899–908.
(18) Morris, E. J.; Darlow, H. M.; Peel, J. F.; Wright, W. C. The quantitative assay of mono-dispersed aerosols of bacteria and bacteriophage by electostatic precipitation. *J. Hyg. (Lond.)* **1961**, *59*, 487–496.
(19) Jang, J.; Akin, D.; Bashir, R. Effects of inlet/outlet configurations on the electrostatic capture of airborne nanoparticles and viruses. *Meas. Sci. Technol.* **2008**, *19*, 1–8.
(20) Kulkarni, P.; Namiki, N.; Otani, Y.; Biswas, P. Charging of particles in unipolar coronas irradiated by in-situ soft X-rays: Enhancement of capture efficiency of ultrafine particles. *J. Aerosol Sci.* **2002**, *33*, 1279–1296.
(21) Watanabe, T.; Tochikubo, F.; Koizumi, Y.; Tsuchida, T.; Hautanen, J.; Kauppinen, E. I. Submicron particle agglomeration by an electrostatic agglomerator. *J. Electrostat.* **1995**, *34*, 367–383.
(22) Yoo, K. H.; Lee, J. S.; Oh, M. D. Charging and collection of submicron particles in two-stage parallel-plate electrostatic precipitators. *Aerosol. Sci. Technol.* **1997**, *27*, 308–323.
(23) Zhuang, Y.; Kim, Y. J.; Lee, T. G.; Biswas, P. Experimental and theoretical studies of ultra-fine particle behavior in electrostatic precipitators. *J. Electrostat.* **2000**, *48*, 245–260.
(24) Hogan, C. J.; Lee, M. H.; Biswas, P. Capture of viral particles in soft X-ray-enhanced corona systems: Charge distribution and transport characteristics. *Aerosol. Sci. Technol.* **2004**, *38*, 475–486.
(25) Jiang, J.; Lee, M. H.; Biswas, P. Model for nanoparticle charging by diffusion, direct photoionization, and thermionization mechanisms. *J. Electrostat.* **2007**, *65*, 209–220.
(26) Shimada, M.; Han, B. W.; Okuyama, K.; Otani, Y. Bipolar charging of aerosol nanoparticles by a soft X-ray photoionizer. *J. Chem. Eng. Jpn.* **2002**, *35*, 786–793.
(27) Peccia, J.; Hernandez, M. Incorporating polymerase chain reaction-based identification, population characterization, and quantification of microorganisms into aerosol science: A review. *Atmos. Environ.* **2006**, *40*, 3941–3961.
(28) An, H. R.; Mainelis, G.; White, L. Development and calibration of real-time PCR for quantification of airborne microorganisms in air samples. *Atmos. Environ.* **2006**, *40*, 7924–7939.
(29) Pyankov, O. V.; Agranovski, I. E.; Pyankova, O.; Mokhonova, E.; Mokhonov, V.; Safatov, A. S.; Khromykh, A. A. Using a bioaerosol personal sampler in combination with real-time PCR analysis

for rapid detection of airborne viruses. *Environ. Microbiol.* **2007**, *9*, 992–1000.
(30) Wang, S. C.; Flagan, R. C. Scanning electrical mobility spectrometer. *J. Aerosol Sci.* **1989**, *20*, 1485–1488.
(31) Hogan, C. J.; Kettleson, E. M.; Lee, M. H.; Ramaswami, B.; Angenent, L. T.; Biswas, P. Sampling methodologies and dosage assessment techniques for submicrometre and ultrafine virus aerosol particles. *J. Appl. Microbiol.* **2005**, *99*, 1422–1434.
(32) U.S.EPA. Method 1602: Male-specific (F^+) and somatic coliphage in water by single agar layer (SAL) procedure; Washington, DC, 2001.
(33) Sambrook, J.; Maniatis, T.; Fritsch, E. F. *Molecular Cloning: A Laboratory Manual*, 2nd ed.; Cold Spring Harbor Laboratory Press: Cold Spring Harbor, NY, 1989.
(34) Golmohammadi, R.; Valegard, K.; Fridborg, K.; Liljas, L. The refined structure of bacteriophage MS2 at 2.8 Å resolution. *J. Mol. Biol.* **1993**, *234*, 620–639.
(35) Shin, G. A.; Sobsey, M. D. Reduction of norwalk virus, poliovirus 1, and bacteriophage MS2 by ozone disinfection of water. *Appl. Environ. Microbiol.* **2003**, *69*, 3975–3978.
(36) Eichwald, O.; Guntoro, N. A.; Yousfi, M.; Benhenni, M. Chemical kinetics with electrical and gas dynamics modelization for NOX removal in an air corona discharge. *J. Phys. D: Appl. Phys.* **2002**, *35*, 439–450.
(37) Mikoviny, T.; Kocan, M.; Matejcik, S.; Mason, N. J.; Skalny, J. D. Experimental study of negative corona discharge in pure carbon dioxide and its mixtures with oxygen. *J. Phys. D: Appl. Phys.* **2004**, *37*, 64–73.
(38) Simek, M.; Clupek, M. Efficiency of ozone production by pulsed positive corona discharge in synthetic air. *J. Phys. D: Appl. Phys.* **2002**, *35*, 1171–1175.
(39) Skalny, J. D.; Matejcik, S.; Mikoviny, T.; Eden, S.; Mason, N. J. Ozone generation in a negative corona discharge fed with N_2O and O^{-2}. *J. Phys. D: Appl. Phys.* **2004**, *37*, 1052–1057.
(40) Huang, S. H.; Chen, C. C. Loading characteristics of a miniature wire-plate electrostatic precipitator. *Aerosol. Sci. Technol.* **2003**, *37*, 109–121.
(41) Kuzmanovic, D. A.; Elashvili, I.; Wick, C.; O'Connell, C.; Krueger, S. Bacteriophage MS2: Molecular weight and spatial distribution of the protein and RNA components by small-angle neutron scattering and virus counting. *Structure* **2003**, *11*, 1339–1348.
(42) Peabody, D. S.; Ely, K. R. Control of translational repression by protein-protein interactions. *Nucleic Acids Res.* **1992**, *20*, 1649–1655.
(43) Stockley, P. G.; Stonehouse, N. J.; Valegard, K. Molecular mechanism of RNA phage morphogenesis. *Int. J. Biochem* **1994**, *26*, 1249–1260.
(44) Atkins, J. F.; Steitz, J. A.; Anderson, C. W.; Model, P. Binding of mammalian ribosomes to MS2 phage RNA reveals an overlapping gene encoding a lysis function. *Cell* **1979**, *18*, 247–256.
(45) Fiers, W.; Contreras, R.; Duerinck, F.; Haegeman, G.; Iserentant, D.; Merregaert, J.; Min Jou, W.; Molemans, F.; Raeymaekers, A.; Van den Berghe, A.; Volckaert, G.; Ysebaert, M. Complete nucleotide sequence of bacteriophage MS2 RNA: Primary and secondary structure of the replicase gene. *Nature* **1976**, *260*, 500–507.
(46) Goodman, N.; Hughes, J. F. The effect of corona discharge on Der p 1. *Clin. Exp. Allergy* **2002**, *32*, 515–519.
(47) Goodman, N.; Hughes, J. F. The effect of corona discharge on dust mite and cat allergens. *J. Electrostat.* **2004**, *60*, 69–91.
(48) Kawamoto, S.; Oshita, M.; Fukuoka, N.; Shigeta, S.; Aki, T.; Hayashi, T.; Nishikawa, K.; Ono, K. Decrease in the allergenicity of Japanese cedar pollen allergen by treatment with positive and negative cluster ions. *Int. Arch. Allergy Immunol.* **2006**, *141*, 313–321.

ES803289W